HHS Public Access

Author manuscript

Nature. Author manuscript; available in PMC 2022 September 12.

Published in final edited form as:

Nature. 2020 June ; 582(7812): 395–398. doi:10.1038/s41586-020-2348-z.

Potential circadian effects in translational failure for neuroprotection

Elga Esposito[1,*], **Wenlu Li**[1,*], **Emiri Tejima-Mandeville**[1,*], **Ji-Hyun Park**[1,2], **Ikbal Sencan**[3], **Shuzhen Guo**[1], **Jingfei Shi**[1,4], **Jing Lan**[1,4], **Janice Lee**[1], **Kazuhide Hayakawa**[1], **Sava Sakadzic**[3], **Xunming Ji**[4], **Eng H. Lo**[1,+]

[1]Neuroprotection Research Laboratories, Departments of Radiology and Neurology, Massachusetts General Hospital, Harvard Medical School, Boston, MA 02129, USA

[2]College of Pharmacy and Research Institute of Pharmaceutical Sciences, Seoul National University, Seoul, 08826, Korea

[3]Athinoula Martinos Center for Biomedical Imaging, Department of Radiology, Massachusetts General Hospital, Harvard Medical School, Boston, MA 02129, USA

[4]Cerebrovascular Research Institute, XuanWu Hospital, Capital Medical University, Beijing, China

Abstract

Neuroprotectants have worked in rodent models but failed in clinical stroke trials. Here, we asked whether opposite circadian cycles in nocturnal rodents versus diurnal humans[1,2] may contribute to this failure in translation. We tested 3 independent neuroprotective approaches in mouse and rat models of focal cerebral ischemia – normobaric hyperoxia, the free radical scavenger αPBN, and the N-Methyl-d-aspartic acid (NMDA) antagonist MK801. All 3 treatments reduced infarction in day-time (inactive-phase) rodent models. All 3 treatments failed in night-time (active-phase) rodent models that match awake day-time patients who are recruited into clinical trials. Laser-speckle imaging showed that the penumbra was narrower in active-phase compared to inactive-phase mice. The smaller penumbra was associated with a lower density of terminal deoxynucleotidyl transferase dUTP nick end labeling (TUNEL)-positive dying cells and reduced infarct growth from 12 to 72 hrs. After inducing circadian-like cycles in primary mouse neurons, oxygen-glucose deprivation triggered a smaller release of glutamate and reactive oxygen species (ROS) as well as a lower activation of apoptotic and necroptotic mediators in "active-phase" versus "inactive-phase" rodent neurons. αPBN and MK801 reduced neuronal death only in "inactive-phase" neurons. These findings suggest that the influence of circadian rhythm on neuroprotection must be considered for translational studies in stroke and central nervous system (CNS) disease.

[+]Corresponding author: Eng H. Lo, Lo@helix.mgh.harvard.edu.
[*]Equal contribution for first 3 authors

AUTHOR CONTRIBUTIONS: Performed experiments and/or analyzed data (EE, WL, ETM, JHP, IS, SG, JS, JL, JL, KH); designed experiments (EE, WL, ETM, JHP, IS, SS, EHL); wrote and/or revised manuscript (EE, WL, ETM, KH, XJ, EHL); funding and support (JHP, SS, XJ, EHL).

Competing Interests: The authors declare they have no competing financial interest.

Circadian rhythm affects mechanisms of disease and response to therapies[1,2]. In stroke, almost all experimental testing of neuroprotectants are performed during the day-time when rodents are normally inactive. In contrast, clinical trials mostly recruit active patients with day-time strokes because of the need to establish time-of-onset. In 5 large clinical trials of neuroprotection in ischemic stroke comprising 9,560 patients, only 664 were night-time strokes (between 10 PM and 7 AM)[3]. Is it possible that animal models mimic non-awake (inactive phase) strokes whereas clinical trials test neuroprotection in awake (active phase) strokes (Figure 1a)?

We first assessed normobaric hyperoxia (NBO), a therapy that worked in rodents but did not succeed in clinical trials[4]. Male Sprague-Dawley rats were subjected to 100 min transient occlusion of the middle cerebral artery, treated with 100% O_2 (NBO) or 30% O_2 (controls), then brains were removed at 24 hrs. NBO reduced infarction when experiments were performed during the day-time (inactive phase, zeitgeber ZT3-9) (Figure 1b). However, NBO did not reduce infarction when experiments were performed at night (active phase, ZT15-21) (Figure 1b). It was noted that infarcts tended to be smaller during the active phase. So, one possibility for the lack of neuroprotection might be because infarcts were already minimal and no further protection was possible. To control for this, we repeated experiments with a less severe 60 min model of transient ischemia. Untreated infarcts were now even smaller but NBO was still able to reduce infarction at ZT3-9 (Figure 1c).

A caveat with the NBO experiments was that the operator was not blinded to day versus night groups, and there was a possibility of decrements in operator performance during night-time surgeries. To account for these issues, animals were housed in normal or reversed light schedule rooms for 3 weeks, and then all surgeries were blindly performed during the day-time. A different operator performed surgeries, a different species was used, and a different neuroprotectant was tested. C57Bl6 male mice were subjected to transient occlusion of the middle cerebral artery for 60 min, then treated with the free radical scavenger αPBN[5] or vehicle immediately and 2 hours after reperfusion. αPBN reduced 3-day infarct volumes in mice during the inactive (ZT3-9) but not active phase (ZT15-21) (Figure 1d).

To assess generalizability, a third series of experiments was performed using a different model and neuroprotectant. C57Bl6 mice from normal or reversed light schedule rooms were subjected to permanent ischemia by coagulating and cutting the distal middle cerebral artery. Mice were treated with the NMDA receptor antagonist MK801[6] or vehicle at 1 hour before ischemia onset. MK801 reduced 3-day infarct volumes during the inactive (ZT3-9) but not active phase (ZT15-21) (Figure 1e). In summary, 3 mechanistically independent, experimentally-proven but clinically-failed neuroprotectants all worked in ZT3-9 but not in ZT15-21 models. These results suggest that neuroprotection may be more difficult to achieve in active rodent models that correspond to day-time patients typically recruited to clinical stroke trials.

In contrast to failures in neuroprotection[7], clinical trials have been positive for thrombolysis and thrombectomy[8,9], implying that reperfusion is a powerful treatment that works in both awake (active) and non-awake (inactive) strokes. C57Bl6 mice from normal or reversed light

schedule rooms were subjected to middle cerebral artery occlusion, then randomized into permanent ischemia or 60 min transient ischemia. In this “positive control” experiment, reperfusion decreased 24 hr infarct volumes in both ZT3-9 and ZT15-21 mice (Figure 1f). Circadian cycles may influence blood hemostasis pathways[10]. Therefore, we checked the clot lysis capacity of tissue plasminogen activator (tPA). There were no significant differences in tPA-clot lysis rates in ZT3-9 versus ZT15-21 mouse blood (Extended Data 2).

Although our studies attempted to cover multiple models and targets, the importance of drug-specific and model-specific effects must be acknowledged. For example, is it possible that by ameliorating reperfusion injury[11], αPBN can affect reperfusion blood flow differently in active versus inactive mice? C57Bl6 mice were subjected to 60 min transient focal ischemia, then treated with αPBN or vehicle immediately and 2 hours after reperfusion. Laser Doppler flowmetry showed no significant differences in reperfusion profiles across all groups (vehicle versus αPBN or ZT3-9 versus ZT15-21; Extended Data 3). For MK801, neuroprotection may be mediated by hypothermia[12]. Is it possible that MK801 affects temperature differently in active versus inactive mice? C57Bl6 mice were treated with MK801 or vehicle, then the distal middle cerebral artery was occluded. There were no significant differences in rectal temperature across all groups (vehicle versus MK801 or ZT3-9 versus ZT15-21; Extended Data 4). Therefore, within the detection limits of our animal models, our observed circadian differences in αPBN and MK801 might not be confounded by large changes in reperfusion or temperature per se.

The penumbra is the conceptual target for neuroprotection in stroke[13,14]. It comprises areas where blood flow is partially maintained so neurons may transiently survive. Therefore, there may be two potential but not mutually exclusive reasons for our results – the penumbra is smaller and/or the penumbra responds differently to ischemia and neuroprotection when animals are awake and active. To assess the first possibility, C57Bl6 mice from normal or reversed light schedule rooms were subjected to focal ischemia, then laser-speckle imaging was performed at 25 min post-occlusion. As expected, there were blood flow gradients in ipsilateral cortex, ranging from normal levels near midline down to ischemic levels in the core (Figure 2a). However, perfusion gradients were steeper in ZT17-19 versus ZT5-7 mice (Figure 2a-b). The ischemic penumbra (areas with intermediate perfusion between 30-50% of normal baseline[15,16]) was narrower in ZT17-19 versus ZT5-7 mice (Figure 2b-c, Extended Data 6).

Without effective treatment, the penumbra collapses and infarction grows. Therefore, another corollary of a smaller penumbra is that there should be less progressive cell death and reduced infarct growth after stroke onset. C57Bl6 male mice from normal or reversed light schedule rooms were subjected to 60 min transient focal ischemia. As expected, infarct volumes grew from 12 to 72 hrs, but the rate of infarct growth was reduced in ZT15-21 versus ZT3-9 mice (Figure 2d), consistent with a smaller penumbra. At 24 hrs post-ischemia, the density of peri-infarct TUNEL-positive cells and the ratio of TUNEL to Fluoro-Jade-positive neurons were lower in ZT15-21 versus ZT3-9 penumbras (Figure 2e-f). Altogether, these results demonstrate that there is a smaller penumbra with less active cell death and reduced infarct growth in ZT15-21 mouse stroke models. These findings indirectly

suggest that there may be less “room to treat” in active rodent models that match day-time stroke patients in neuroprotection trials.

Central circadian control resides in the suprachiasmatic nucleus but circadian rhythms may also occur in cortex[17,18]. We dissected somatosensory cortex from C57Bl6 mice and Sprague-Dawley rats, and measured representative circadian genes with RT-PCR. Our data confirmed that in this area commonly affected in stroke, the temporal profile of circadian genes in mice and rats appears opposite to human and nonhuman primate brain, consistent with the fact that rodents are nocturnal animals (Extended Data 7). Is it possible that circadian cycles may also directly affect the neuronal susceptibility to ischemia and response to neuroprotection per se?

Dexamethasone was used to trigger circadian-like Per1/Per2 cycles in primary mouse cortical neurons[19] (Figure 3a). These cycles allowed us to mimic in vivo experiments performed in active phase (6 hrs post-dexamethasone, high Per1/Per2) versus inactive phase (12 hrs post-dexamethasone, low Per1/Per2). Neurons were subjected to 3 hrs oxygen-glucose deprivation and re-oxygenated for 24 hrs, then cell viability assays were performed to quantify neuroprotection (Figure 3b). Oxygen-glucose deprivation for 3 hrs led to 30-40% neuronal cell death. Although effect sizes were small, αPBN and MK801 appeared to significantly reduce cell death in “inactive phase” but not “active phase” rodent neurons (Figure 3c-d).

Since it was more difficult to protect “active phase” versus “inactive phase” neurons, we looked for differences in “targetable mechanisms”. After oxygen-glucose deprivation, glutamate release and ROS levels increased. However, glutamate and ROS elevations were smaller in “active” versus “inactive” neurons (Figure 3e), suggesting that excitotoxicity and oxidative stress may be less prominent and therefore less therapeutically relevant in “active” rodent neurons. Next, we looked at downstream cell death mechanisms including apoptosis and necroptosis[20]. Oxygen-glucose deprivation induced activation of caspase-3 and RIP3 kinase, but these responses were also smaller in “active” versus “inactive” rodent neurons (Figure 3f-h). After cerebral ischemia, neurons die via both passive and active cell death modes[21]. The former is a “dissipative” cell death that occurs after severe loss of oxygen and glucose leading to metabolic collapse. These processes may occur in the core, and can only be blocked by prompt return of missing energy substrates. The second is an “active” mode that recruits upstream excitotoxicity and oxidative stress, and downstream apoptosis and necroptosis. This “active” cell death is the conceptual target of molecular neuroprotection, presumably within the penumbra. Therefore, our in vitro results may be consistent with the in vivo findings of less active cell death and decreased infarct growth in ZT15-21 versus ZT3-9 stroke models, thus implying that there should be less “targetable injury” in ZT15-21 rodent models that match day-time stroke patients. A final proof-of-concept experiment was performed to examine this “resistance to neuroprotection”. Although it is impossible to block everything, we attempted to cover as many aspects of active cell death as possible: MK801 to block NMDA excitotoxicity, NBQX to block AMPA excitotoxicity, αPBN to block ROS, zVAD-fmk to block apoptosis, and Necrostatin-1 to block necroptosis. Consistent with observed differences in active cell death, “resistance to neuroprotection”

(i.e. injury that is left after blocking major active cell death targets) was larger in “active” versus “inactive” rodent neurons (Figure 3i).

Our findings point to a fundamental difference between currently used rodent models of neuroprotection versus human stroke patients. Clinical trials test neuroprotectants in active/awake patients, whereas rodent models are performed during the day-time when they are inactive. Nevertheless, there are caveats that must be kept in mind. First, circadian differences cannot be the only reason for translational failure. Other aspects of rodent models also do not match clinical populations, including age, hypertension and metabolic disease. Indeed, the free radical spin trap NXY-059 was tested in marmosets[22,23] (in 2 studies from a single lab) but still failed in clinical trials. Future studies are warranted to examine how circadian rhythms interact with age and comorbidities. Second, our study suggests that circadian rhythms affect the penumbra but the underlying mechanisms remain to be clarified. How circadian rhythm affects neurovascular coupling in normal versus ischemic tissue should be explored[24-25]. Third, we showed a circadian influence on the neuronal response to oxygen-glucose deprivation. Further studies are needed to dissect how neuroprotection is modulated by crosstalk between circadian genes and cell survival/death genes[26]. Fourth, our in vivo experiments focused on infarction. This approach will not work for drugs that promote recovery. How circadian cycles interact with neuroplasticity should be examined[27]. A fifth issue concerns stress. Although all groups were subjected to uniform handling methods and there were no detectable differences in cortisol (Extended Data 8), circadian differences may also involve unavoidable stress differences in active versus inactive rodents. Finally, circadian biology may interact with multiple aspects of stroke pathophysiology including glial reactions, cytokines/chemokines, endothelial/hemostatic mechanisms, immune response, temperature regulation, blood-brain barrier, and drug delivery/metabolism[28-29]. How these systems differ in active versus inactive rodent models must be investigated.

Failed neuroprotection trials in stroke have led to some pessimism in the field. However, recent successes with thrombectomy and reperfusion have led to calls to resume the quest[30]. This study suggests that in order to move forward, stroke mechanisms and targets should be re-assessed in rodent models with the appropriate circadian context.

DETAILED METHODS:

Animals:

Male Sprague-Dawley rats (320 to 340 g) (Charles River Laboratories, Wilmington, MA) were housed in a room with standard light schedule 12 hours of light (on) during the day (7am-7pm) and 12 hours of dark (off) at night (7pm-7am). Male (C57BL/6J, 25 to 28g) (Charles River Laboratories, Wilmington, MA) were randomly housed for 3 weeks before surgery and 1 or 3 days after surgery in 2 different rooms, one room had standard light schedule 12 hours of light (on) during the day (7am-7pm) and 12 hours of dark (off) at night (7pm-7am) and another room had switched cycle 12 hours of dark (off) during the day (7am-7pm) and 12 hours of light (on) at night (7pm-7am). These acclimatization and handling procedures were uniformly applied for all groups in all surgical, physiology, neuroprotection, gene expression and imaging experiments. However, it is noted that as part

of the differences in circadian context, animals may unavoidably experience different levels of stress when experiments are performed during active/awake versus inactive/non-awake times. Experiments were performed under institutionally approved protocol in accordance with the National Institute of Health's Guide for the Care and Use of Laboratory Animals. All animals were randomly allocated to treatment groups.

Rat and mouse focal ischemia:

All animals were anesthetized with isoflurane (1.5%) in 30%/70% oxygen/nitrous oxide. Transient focal ischemia was induced introducing a 6-0 (in mice) or 5-0 (in rats) surgical monofilament nylon suture (Doccol) from the external carotid artery into the internal carotid artery and advancing it to the branching point of the MCA. Adequate ischemia was confirmed by continuous laser Doppler flowmetry (LDF) (Perimed, North Royalton, OH, U.S.A.). Animals that did not have a significant reduction to less than 30% baseline LDF values during MCAO were excluded. After occluding the MCA for 60 mins in mice and 100 mins in rats, the monofilament suture was gently withdrawn in order to restore blood flow. In mice that underwent to permanent proximal ischemia the filament was left in the artery until the animal was euthanized. Rectal temperature was maintained at 37°C with a thermostat-controlled heating pad.

Rats were randomized into control, 85′NBO groups or 61′NBO groups. The control group received 30% O_2 during all occlusion time. The 85′NBO group received 100% O_2 for 85 mins, from15 mins after MCAO until the end of the occlusion. The 61′NBO group received 100% O_2 for 61 mins, from 9 mins after MCAO until the end of the occlusion. These are based on NBO protocols in the literature that have been shown to work in rodent models [31]. Basically, NBO was induced by exposing animals to 100% inspired oxygen. This is known to raise arterial pO_2 levels above 300 mmHg.

Mice were divided into two groups: MCA occlusion control group, αPBN treatment group. αPBN (100 mg/kg, i.p.) was injected in mice immediately after reperfusion and 2 hours later.

Distal permanent ischemia in mice:

Mice were anesthetized with isoflurane under spontaneous respiration in a nitrous oxide/ oxygen mixture. A burr hole (3 mm diameter) was drilled under saline cooling in the temporal bone overlying the distal MCA. The dura was kept Intact. The exposed artery was occluded with a microbipolar coagulation and cut between the lateral olfactory tract and the inferior cerebral vein.

The animals were divided into two groups: MCA occlusion control group, MK-801 treatment group. In the MK-801 treatment group, MK-801 (2.5 mg/kg) was administered intraperitoneally 1 hour before MCA occlusion.

The exclusion criteria for transient and permanent focal ischemia via intraluminal occlusions of the middle cerebral artery were based on laser doppler flow (LDF; animals that did not have a significant reduction to less than 30% baseline during MCAO or LDF was not recovered to 100% during reperfusion were excluded), surgery failure (i.e. excessive

bleeding during surgery) and animals euthanized for poor health conditions when suggested by veterinary. The exclusion criteria for permanent distal occlusion of the middle cerebral artery were based on surgery failure (i.e. bleeding during surgery, artery occlusion in the wrong position or artery was not properly cut).

Cerebral ischemia, treatments and circadian cycles:

All experiments followed standard protocols for randomization of group assignment via 4 number lottery draw, allocation concealment, blinding of operators, blinding of measurements, blinding of analyses. For a typical experiment, there should be 4 groups: day control, day drug, night control, night drug. Treatment dosing was based on extensive neuroprotection literature. NBO was administered as 100% inspired oxygen that results in arterial pO_2 above 300 mmHg; this approach matches dosing in both experimental models and clinical trials [31]. Our doses of MK801 and αPBN were based on the extensive preclinical neuroprotection literature [32-35]. MK801 was tested in human trials of epilepsy and attention deficit disorders repeated 0.15 mg/kg oral dosing [36]. The related spin trap NXY-059 was tested in stroke patients with iv infusions of 2270 mg (5940 μmol) per hr, reduced after 1 hr to 480 to 960 mg (1260 to 2520 μmol) per hr for a further 71 hrs [37]. Our experiments were intended to test the idea that after cerebral ischemia, response to these 3 potential neuroprotective therapies may be affected by circadian cycles. These studies do not unequivocally define all the ischemia-circadian interaction mechanisms that may be involved [38-43].

Physiological parameters:

Physiological parameters such as blood pressure, pH, pCO_2, PO_2, glucose and temperature were measured. Before surgery and PBN treatment MAP [mmHg] was measured in awake ZT3-9 and ZT15-21 mice. For PBN treatment groups the right femoral artery was cannulated with PE-10 polyethylene tubing and blood was collected 30 mins after occlusion, 10 mins after reperfusion and first drug injection and 24 hrs later (22hrs after drug injection). For MK801 treatment groups arterial blood was collected as well from the right femoral artery at 1 hr after distal permanent occlusion (2 hrs after drug injection), and 24 hrs later (25 hrs after drug injection). In all groups, before collecting blood, at the same time points, blood pressure was measured. Body temperature was measured with a rectal temperature probe. Insulin and cortisol measurements were performed with the Ultra Sensitive Mouse Insulin ELISA Kit (Crystal Chem USA, Elk Grove Village, IL, U.S.A.) and Cortisol ELISA Kit (Enzo, Farmingdale, NY, U.S.A.) after blood withdrawn from the posterior vena cava.

Speckle imaging:

Mice were anesthetized and focal ischemia was performed by filament model. To minimize the breathing motion, the animal head was restrained in a stereotaxic frame by using the ear bars. The scalp and the overlying membrane from the skull were gently incised down the midline and peeled to the side. The systemic arterial blood-gas measurement was performed at the end of each experiment to record pCO_2 and blood pressure (Extended Data 5). A laser diode (780 nm) was used for illumination and laser speckle images were recorded by using a CMOS camera (acA1300-200μm, Basler), 25 mins post-occlusion. For each animal, three sets of raw speckle images were acquired in <15 s (300 frames in each

set; image width = 1280; image height = 1024; pixel size = 11.72 μm; exposure time = 5 ms). A speckle contrast image was calculated from each raw speckle image using a sliding grid of 7×7 pixels. A mean speckle contrast image was calculated for each set and used to calculate the decorrelation time and relative cerebral blood flow (rCBF) at each pixel. The relative cerebral blood (rCBF) in the ipsilateral (ischemic) hemisphere was normalized by the mean rCBF in the contralateral (non-ischemic) hemisphere. The mean lateral-medial profile of the rCBF was computed for the 4.1-0.6 mm range from the midline, within a coronal band between lambda and bregma. We defined the ischemic penumbra as the cortical territory with the rCBF values between 30-50% of baseline and estimated the width of penumbra based on the mean lateral-medial rCBF profile. These steps were repeated for each acquisition set. These thresholds were based on operational definitions proposed by Heiss and Hossmann [15-16]. The ischemic threshold for infarction (i.e. the core) is approximately 20-25 mL/100g/min. The threshold for gene expression and protein synthesis inhibition (i.e. upper limit for penumbra) is approximately 50-60 mL/100g/min. Based on rodent CBF values of approximately 110-120 mL/100g/min, this corresponded to a penumbral range of 30-50%. Speckle imaging data were also expressed as absolute flow values by first confirming that mean speckle decorrelation times were similar in healthy mice and in the nonischemic hemisphere of mice with focal ischemia (t_c=52.8±14.3 and 61.2±18.6, mean ± SD respectively), then recalculating all data based on 115 mL/100g/min in mouse cortex. CBF data from all pooled hemispheres were plotted as histograms, and then thresholded to areas between 25-55 mL/100g/min in individual mice for penumbral comparisons between day-time versus night-time mice. All analysis was done by using a custom script written in MATLAB (MathWorks). All analyses were randomized and blinded.

Evaluation of infarct volume:

The animals underwent transcardial perfusion with saline after 1 or 3 days after ischemia. Brains were quickly removed placed within a brain matrix and cut in 7 (in rats) or 8 (in mice) coronal sections. The sections were then incubated in 2% TTC in saline for 10 min at room temperature. Infarction volumes were quantified using the “indirect” morphometric method with Image J software. All analyses were blinded.

Primary neuron cultures and circadian gene induction.

Primary neuron cultures were prepared from the cortex of embryonic day (E)17 C57BL/6 mice embryos (Charles River Laboratory). Briefly, the cortical tissues were dissected and digested with Trypsin (Invitrogen). The cells were then plated onto poly-D-lysine-coated plates at a density of 3×10^5 cells/ml and cultured in DMEM (Life Technology, 11965-084) containing 5% fetal bovine serum (FBS). After 24 h, the medium was changed to NeuroBasal medium (Invitrogen, 21103-049) supplemented with 2% B-27 (Invitrogen, 17504044), 0.5 mM L-glutamine and 1% penicillin-streptomycin and replaced every 2-3 days. The neuron cells were cultured in humidified incubator at 37°C and 5% CO_2 and were used for experiments from 8 to 11 days in vitro. To induce the circadian gene expression, neuron cultures were stabilized without changing media for 4 days, then dexamethasone (100 nM) was added and incubated for 2 hrs, after which the media was replaced with regular NeuroBasal media. Cells were then harvested or subjected to OGD at indicated time

points. These cell culture experiments only attempt to mimic circadian cycles which is by definition, is a whole organism in vivo phenomenon. However, these experiments may build on previous literature that have investigated the interactions between circadian genes and neuronal injury [26, 43-45].

RT-PCR.

Total mRNA was extracted using QIAzol lysis reagent (QIAGEN, 79306) and reverse transcribed using High-Capacity RNA-to-cDNA™ Kit (Thermo Fisher Scientific, 4387406) according to the manufacturer's instructions. The relative transcript level of circadian genes was measured by Real Time PCR system (Applied Biosystems) using each primer of Per1 (Applied Biosystems, Mm00501813), Per2 (Mm00478099), TBP (Mm01277042), and HPRT1 (Mm01545399). Fold change in transcript level was calculated by ΔΔCt normalized to 0 time samples.

Oxygen-glucose deprivation (OGD) and reoxygenation.

To induce OGD, the culture medium was replaced with deoxygenated, glucose-free DMEM (Life Technology, 11966-025) with or without neuroprotective reagents, MK-801 (10 μM) or aPBN (1μM), and cells were placed in a humidified chamber (Heidolph, incubator 1000, Brinkmann Instruments) which was perfused with anaerobic gas mixture (90% N_2, 5% H_2, and 5% CO_2) for 30 mins, then sealed and kept at 37°C. After 2 hrs (αPBN) or 3 hrs (MK-801) of OGD, cultures were removed from the anaerobic chamber, and the media was replaced with NeuroBasal media supplemented with B-27 Minus AO (Invitrogen, 10889038) with or without the neuroprotective reagents. Cells were then allowed to recover for 24 hrs for cell viability assay in a regular incubator.

Cell viability assays.

Neuron cell injury was assessed by lactate dehydrogenase (LDH) assay using the Cytotoxicity Detection Kit (Roche Applied Science, 11644793001) according to the manufacturer's instructions. Briefly, 500 μl of medium was collected and then centrifuged for 5 mins at 500 g. 50 μl of supernatant was transferred to a 96-well plate in triplicate and 50 μl of dye/catalyst solution was added. The assay plates were then incubated at room temperature in the dark for 20 mins and then were read the absorbance at 490 nm. For MTT assay (Sigma, M2128), MTT reagent (final concentration 0.5 mg/ml) was added to neurons in 24-well plates and incubated at 37°C for 1 hr, then 200 μl of DMSO was added to solubilize the purple formazan. The absorbance was measured at 570 nm using a microplate reader. The relative assessments of neuronal injury were normalized by comparison with control cells as 100% cell survival.

Glutamate and ROS release assays.

Glutamate production was measured by Glutamate Assay Kit (Cell Biolabs, MET-5080). Briefly, neuron cell culture supernatants were centrifuged at 10,000 rpm for 5 mins to remove insoluble particles. Add 50 μl of Glutamate standard or each sample into wells of a 96 well plate. Then add 200 μl of Reaction Mix/Control Mix to the wells, and mix the well contents thoroughly. Incubate at room temperature for 60 mins on an orbital shaker. Read

absorbance of each well on a microplate reader using 450 nm as the primary wave length. ROS detection was measured by the carboxy derivative of fluorescein- carboxy-H2DCFDA (C400) which carries additional negative charges that improve its retention compared to noncarboxylated forms. Briefly, neuron cell culture supernatants were removed. Cells were incubated in pre-warmed Hanks' balanced salt solution (HBSS) containing the probe to provide a final working concentration of 5 μM dye for 30 mins. Then HBSS was removed, cells were returned to pre-warmed media and incubated at the 37°C for different time. The baseline fluorescence intensity of the loaded cells was determined prior to exposing the cells to experimental inducements. These glutamate and ROS measurements were intended as indirect in vitro markers to support the overall idea of "larger active cell death mechanisms in larger penumbras during active-phase strokes". A recent human study showed that higher plasma levels of oxidative stress biomarkers were indeed correlated with larger diffusion-perfusion MRI mismatch penumbras[46].

In Vitro interaction of tPA and blood clots.

Blood clots were prepared with 100 μl of heart ventricle blood. After 45 min of maturation at 37°C with continuous shaking at 50 rpm, clots were moved from each Eppendorf tube into a 24-multiwell dish with 1.5 mL of saline solution for each well. Dissolution rates of blood clots were measured estimating the amount of hemoglobin released from the clots over time. Clots were treated with 30 μg of tPA/clot. Clots were incubated at 37°C with continuous shaking at 50 rpm for 180 mins. At times 0, 30, 90, 180 mins post- treatment, 200 μl of supernatant was placed in a 96-multiwell dish, and the optical density (OD 415) of the hemoglobin released in the dissolution was measured in a microplate reader. The dissolution rate (DR) was measured with the following formula: $DR = (ODi - OD0)/(ti - t0)$ where i and 0 are two consecutive time points.

Immunohistochemistry.

Samples were initially fixed with 4% paraformaldehyde for 10 mins at room temperature. Then, samples were processed with 0.1% Triton X for 5 mins, followed by 5% BSA blocking for 1 hr at room temperature. The slides were then transferred to the TUNEL (Biotium, 30074) working solution for 1 hr at 37 °C and then rinsed. To combine with Fluoro-Jade, the slides were then transferred to the Fluoro-Jade (Sigma, AG325) working solution for 10 mins and then rinsed, air dehydrated, xylene cleared. Nuclei were counterstained with 4,6-diamidino-2-phenylindole (DAPI), and coverslips were placed. Immunostaining images were obtained with a fluorescence microscope (Nikon ECLIPSE Ti-S) or Nikon A1SiR Confocal Microscope.

Western blot analysis.

Protein samples were loaded onto 4–12% Tris-glycine gels. After electorophoresis and transferring to nitro-cellulose membranes, the membranes were blocked in Tris-buffered saline containing 5% no-fat milk for 60 mins at room temperature. Membranes were then incubated overnight at 4°C with antibodies against Caspase3 (Cell Signaling Technology, 9662S), cleaved-Caspase-3 (Cell Signaling Technology, 9661S), RIP3 (Cell Signaling Technology, 95702), and Phospho-RIP3 (Thr231/Ser232) (Cell Signaling Technology, 57220). After incubation with peroxidase-conjugated secondary antibodies, visualization

was enhanced by chemiluminescence (GE Healthcare, NA931- anti-mouse, or NA934-anti-rabbit). Optical density was assessed using the NIH Image analysis software.

Cell Resistance.

Cell counting kit (CCK)-8 (Dojindo) was used for the determination of the number of viable cells. Briefly, 20 ul reagent was added to mouse neuron cultures in 48-well plates at 37°C for 1 h. The plates were then read using a standard plate reader with a reference wavelength of 450 nm. Background values from 630 nm were subtracted from those of 450 nm. The resistance of cells was measured with the following formula: Resistance (%) = [1-OGD_{drug}/Con_{drug}]/[1-OGD_{dmso}/Con_{dmso}]*100%.

Statistical analysis:

Results were expressed as mean ± SEM. All experiments were performed with randomization of group assignment via 4 number lottery draw, allocation concealment, blinding of operators, blinding of measurements, and blinding of analyses. When only two groups were compared, unpaired two-tailed t-test was used. Multiple comparisons were evaluated by one-way or two-way ANOVA (with repeated measures when appropriate) followed by Tukey-Kramer tests or Bonferoni corrections. P values of $p<0.05$ were considered statistically significant.

Extended Data

Extended Data 1:

Physiologic parameters, laser doppler flow, mortality, inclusion/exclusions for neuroprotection experiments in Figure 1. All values are mean ± SEM.

	ZT 3-9		ZT 15-21	
Mouse (n)	**Control**	**PBN**	**Control**	**PBN**
Total surgery	19	17	19	21
Total included	11	15	12	13
Excluded	3/19	0/17	4/19	6/21
Mortality	5/19	2/17	3/19	2/21
	ZT 3-9		**ZT 15-21**	
Mouse (n)	**Control**	**MK801**	**Control**	**MK801**
Total surgery	17	15	16	21
Total included	15	12	13	11
Excluded	2/17	3/15	3/16	9/21
Mortality	0/17	0/15	0/16	1/21
	ZT 3-9		**ZT 15-21**	
Rat (n)	**Control**	**NBO 85’**	**Control**	**NBO 85’**
Total surgery	24	21	15	16
Total included	15	13	12	12
Excluded	8/24	8/21	3/15	4/16
Mortality	1/24	0/21	0/15	0/16

	ZT 3-9		ZT 15-21	
Mouse (n)	**Control**	**PBN**	**Control**	**PBN**

	ZT 3-9		ZT 15-21	
Mouse (n)	**Permanent**	**Transient**	**Permanent**	**Transient**
Total surgery	18	13	15	16
Total included	11	12	12	12
Excluded	0/18	1/13	0/15	2/16
Mortality	7/18	0/13	3/15	2/16

	ZT 3-9	
Rat (n)	**Control**	**NBO 51’**
Total surgery	18	14
Total included	10	10
Excluded	8/18	4/14
Mortality	0/18	0/14

	ZT 3-9		ZT 15-21	
Mouse	**Control**	**PBN**	**Control**	**PBN**
0 min				
MAP [mmHg]	122±4.4	125±2.4	120±1.7	122±3.3
30 min				
MAP [mmHg]	94.6±5.39	88.3±3.29	87.6±3.40	86.5±3.45
pH	7.33±0.002	7.29±0.071	7.27±0.040	7.39±0.003
pO2 [mmHg]	182±23.4	154.75±12.3	177.5±11.9	185.8±15.4
pCO2 [mmHg]	40.2±1.80	40.5±3.63	46.6±5.32	35.4±1.14
Glu [mg/dL]	230.3±11.1	290±35.8	162.2±42.2	164.8±8.9
T [°C]	37.2±0.22	37.2±0.04	37.1±0.19	37.3±0.13
70 min				
MAP [mmHg]	89.5±2.39	82.3±2.57	85.7±2.25	79.5±2.5
pH	7.31±0.015	7.18±0.081	7.31±0.036	7.31±0.012
pO2 [mmHg]	189±23.9	155±15.6	149±26.7	183±15.24
pCO2 [mmHg]	43±0.97	44.8±4.59	43.7±3.85	38.5±1.17
Glu [mg/dL]	244.5±13.7	407.7±44.9	199.8±7.3	144.2±12.5
T [°C]	37.2±0.1	37.3±0.2	37.5±0.1	37.5±0.2
24 h				
MAP [mmHg]	79±6.33	78.7±5.15	77.5±6.81	76.6±3.11
pH	7.37±0.016	7.20±0.062	7.27±0.056	7.13±0.069
pO2 [mmHg]	232±17.4	199±25.6	229.2±7.7	185.7±16.4
pCO2 [mmHg]	34.7±1.4	38.1±3.1	38.1±1.5	46.1±3.2
Glu [mg/dL]	244.5±13.7	407.7±44.9	199.8±7.3	144.2±12.5
Insulin [ng/mL]	0.39±0.09	0.43±0.05	0.35±0.06	0.58±0.15
T [°C]	35.6±0.3	35.6±0.6	35.7±0.1	35.5±0.4

	ZT 3-9		ZT 15-21	
Mouse	**Control**	**MK801**	**Control**	**MK801**

	ZT 3-9		ZT 15-21	
Mouse (n)	**Control**	**PBN**	**Control**	**PBN**
60 min				
MAP [mmHg]	85±2.03	84.25±0.25	84.75±2.46	85.25±2.09
pH	7.35±0.019	7.29±0.019	7.4±0.01	7.33±0.004
pO2 [mmHg]	170±6.39	170±8.17	167.2±7.71	153±8.63
pCO2 [mmHg]	35.6±2.7	39.8±1.5	33.2±2.2	40.1±1
Glu [mg/dL]	327±21.3	343.7±18.3	282.5±27.2	272.8±29.8
Insulin [ng/mL]	0.83±0.12	1.05±0.32	0.64±0.12	0.98±0.28
24 h				
MAP [mmHg]	89.2±2.56	90.7±4.85	84.7±1.44	87.2±1.93
PH	7.41±0.008	7.36±0.01	7.39±0.029	7.37±0.003
pO2 [mmHg]	178.5±19.2	174.2±9.4	181.5±12.3	191.2±15.4
pCO2 [mmHg]	34.6±1.7	38.0±0.9	35.1±1.2	39.7±1.1
Glu [mg/dL]	211.7±10.4	240±30.1	181.2±13.3	199±22.1
Insulin [ng/mL]	0.53±0.12	0.38±0.07	0.84±0.51	0.82±0.26
	ZT 3-9		**ZT 15-21**	
Rat (60 min)	**Control**	**NBO 85’**	**Control**	**NBO 85’**
MAP [mmHg]	101±5.1	108±2.7	98.2±5.7	102.7±10.7
pH	7.45±0.018	7.38±0.003	7.41±0.030	7.40±0.016
pO2 [mmHg]	180±7.4	462.2±11.33	206.2±11.12	468.7±20.03
pCO2 [mmHg]	37.4±2.62	45.5±2.08	41.6±3.03	45.5±3.72
LDF(%)	26±1.64	26.6±1.67	26.2±1.58	26.6±2.45

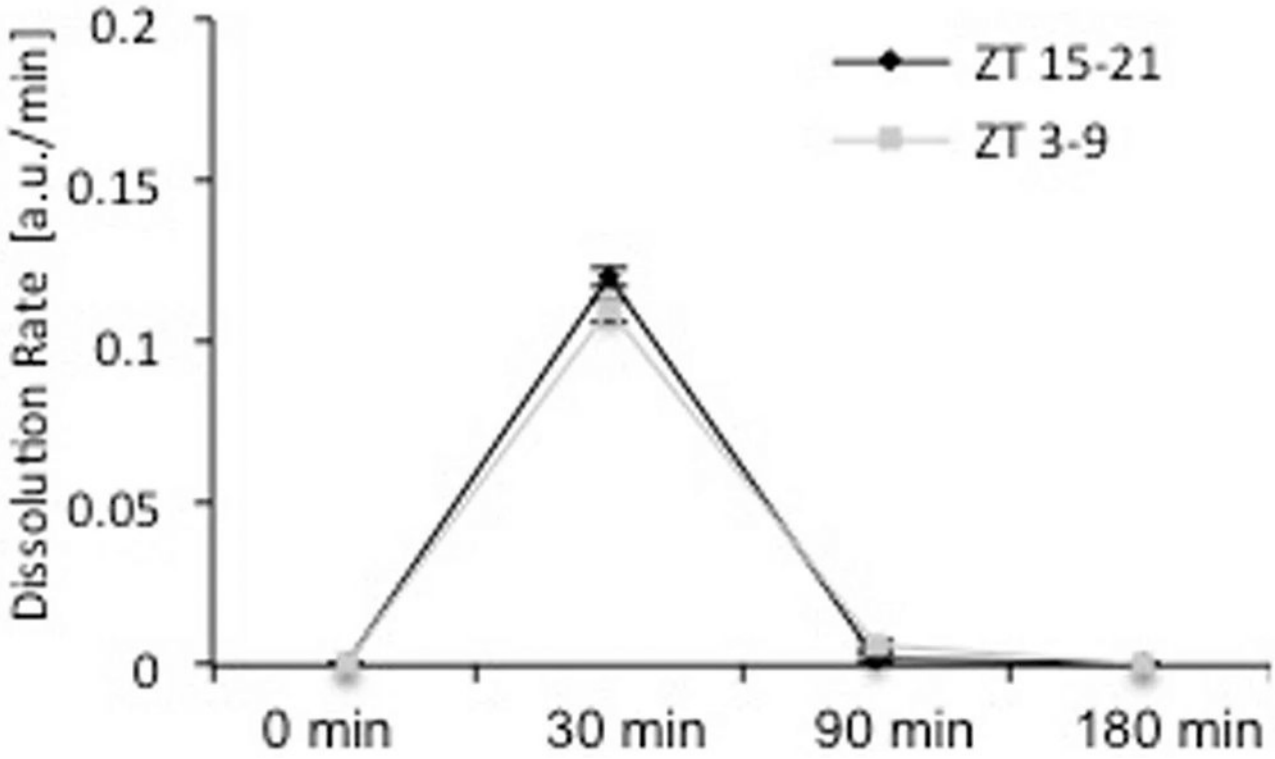

Extended Data 2:

Rates of tissue-plasminogen activator-induced clot lysis were not significantly different in blood drawn from day-time (ZT3-9, n=5) or night-time (ZT15-21, n=8) male C57BL6 mice (mean ± SEM, repeated-measures ANOVA p=0.80).

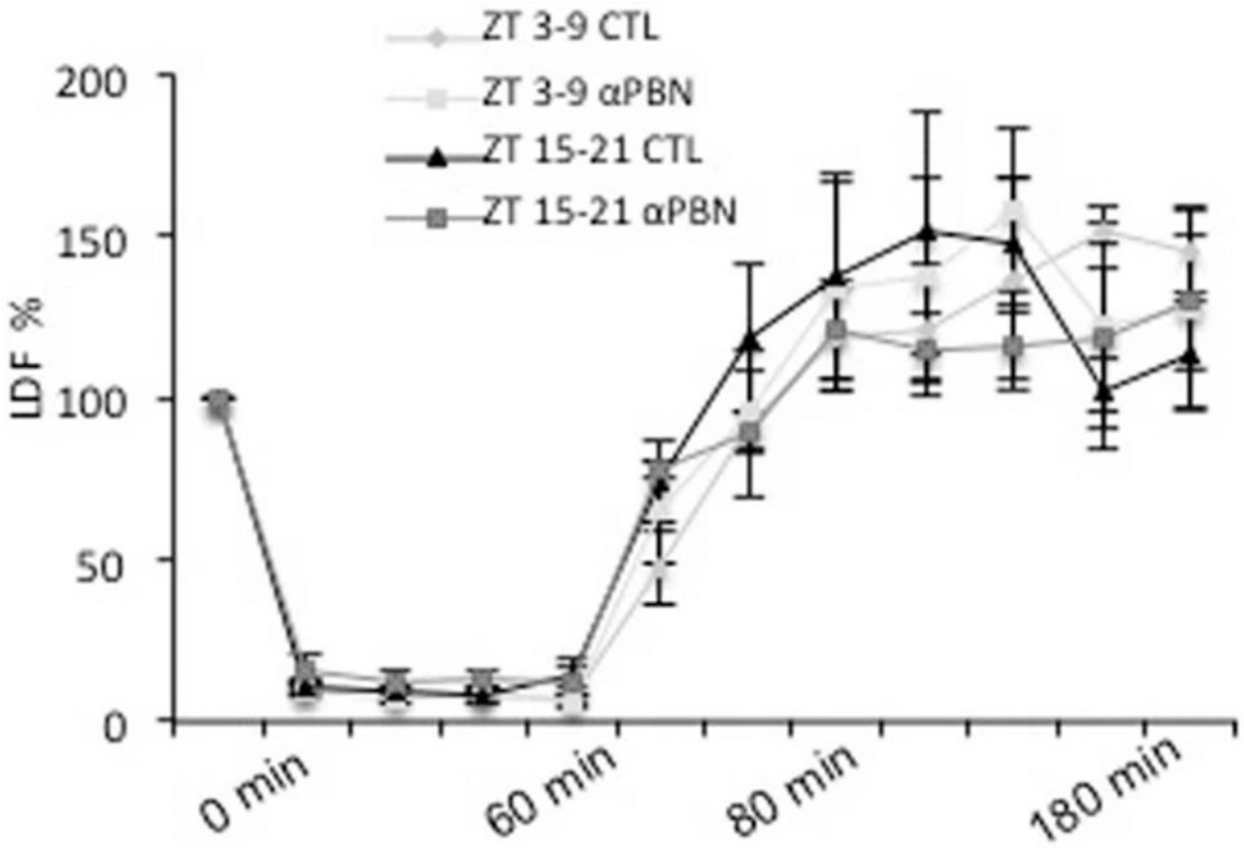

Extended Data 3:

Laser Doppler flowmetry showed that αPBN (100 mg/kg) did not affect reperfusion profiles after 60 min transient focal ischemia in ZT3-9 versus ZT15-21 male C57BL6 mice (mean ± SEM, n=4 per group, repeated-measures ANOVA p=0.87).

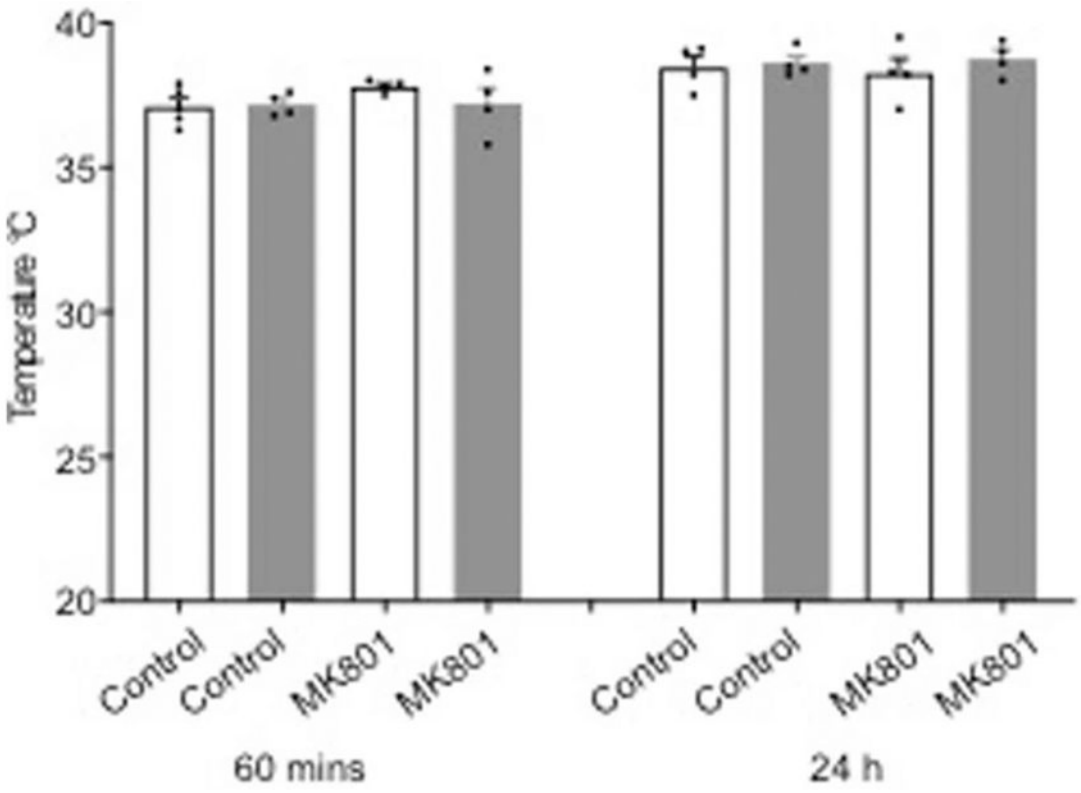

Extended Data 4:
MK801 did not significantly affect body temperature after permanent focal cerebral ischemia in ZT3-9 (white bars) versus ZT15-21 (gray bars) male C57BL6 mice (mean ± SEM, n=4 per group, repeated-measures ANOVA p=0.97).

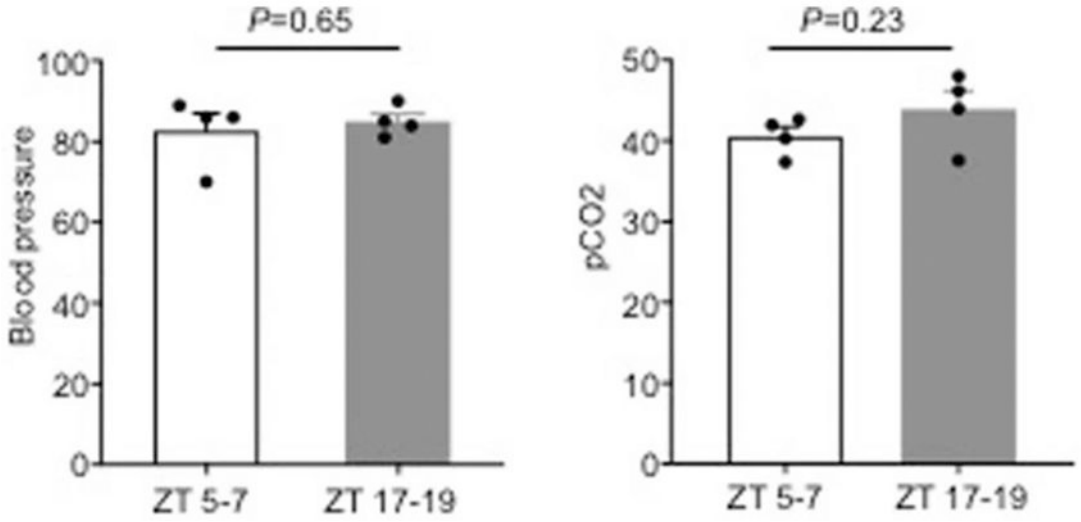

Extended Data 5:
Physiologic parameters for laser speckle imaging experiments in Figure 2 (n=4 mice per group). All values are mean ± SEM, P values in data from 2-tailed t test comparison.

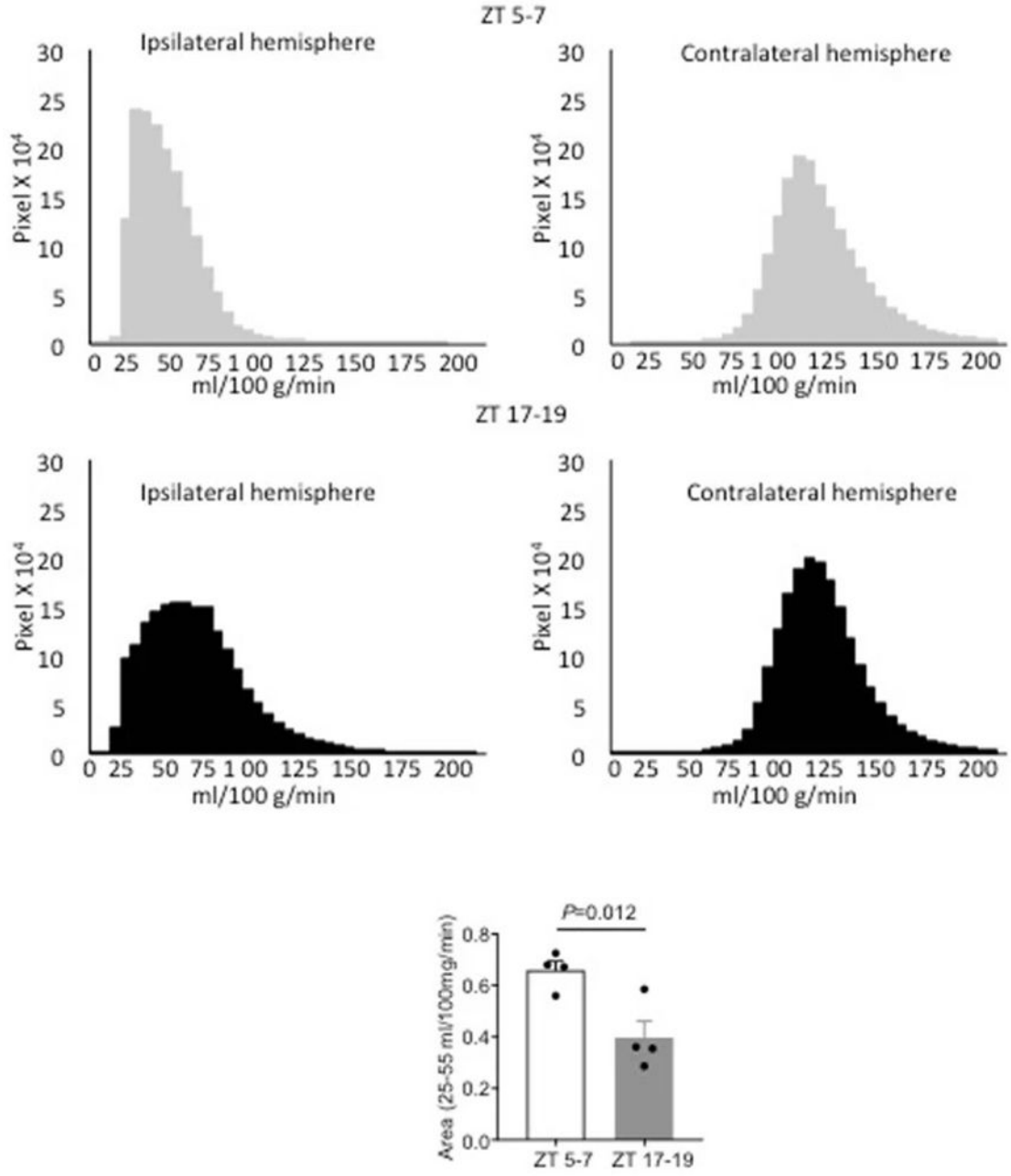

Extended Data 6:

Quantitation of blood flow was checked by calculating speckle imaging data in terms of absolute blood flow (mL/100g/min). Blood flow histograms show the presence of cerebral ischemia in the ipsilateral hemispheres (top panel). Thresholded areas between 25-55 mL/100g/min (see Methods) were significantly smaller in ZT17-19 versus ZT5-7 C57BL6 male mice (n=4 per group, comparisons via 2-tailed t test).

Expression of circadian genes in cortex of rodents and primates

ZT6	MOUSE	RAT	HUMAN/ PRIMATE	ZT18	MOUSE	RAT	HUMAN/ PRIMATE
Per1	⇩	⇩	⇧ *(cit. 17-18)*	Per1	⇧	⇧	⇩ *(cit. 17-18)*
Per2	⇩	⇩	⇧ *(cit. 17-18)*	Per2	⇧	⇧	⇩ *(cit. 17-18)*
Cry1	⇩	⇩	⇧ *(cit. 17)*	Cry1	⇧	⇧	⇩ *(cit.17.)*

Expression of circadian genes in cortex of rodents
(absolute levels relative to housekeeping gene Hprt1)

(n=6)	ZT 5-7		ZT 17-19	
Rat	Mean	SEM	Mean	SEM
Bmal1	0.292	0.008	0.323	0.005
Clock	0.645	0.027	0.796	0.026
Cry1	0.021	0.001	0.049	0.002
Cry2	1.564	0.148	2.117	0.167
Per1	0.735	0.168	1.416	0.146
Per2	0.036	0.004	0.123	0.005

(n=4)	ZT 5-7		ZT 17-19	
Mouse	Mean	SEM	Mean	SEM
Bmal1	0.275	0.020	0.297	0.019
Clock	0.493	0.036	0.512	0.037
Cry1	0.080	0.004	0.128	0.010
Cry2	0.337	0.018	0.354	0.026
Per1	0.562	0.100	0.855	0.063
Per2	0.086	0.009	0.175	0.015

Extended Data 7:

Expression of selected circadian genes in C57BL6 male mouse and Sprague-Dawley male rat somatosensory cortex (n=4 per group), and comparison of circadian gene patterns between mice, rats, nonhuman primates and humans.

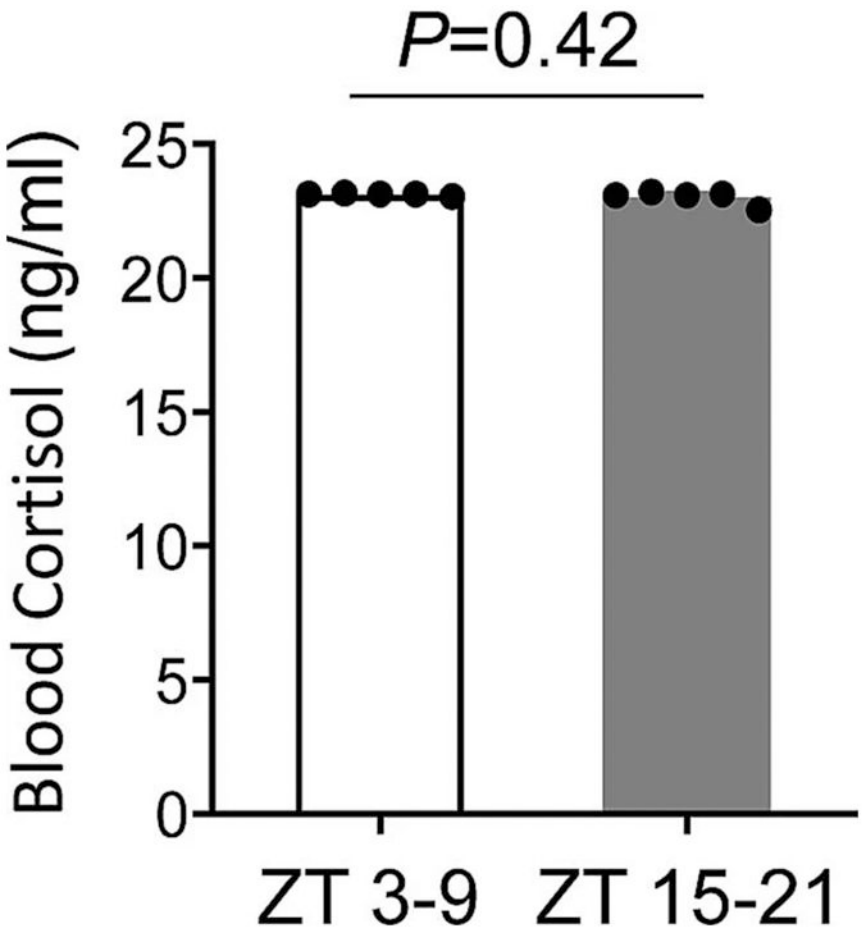

Extended Data 8:
No significant differences were detected in blood cortisol levels of ZT 3-9 versus ZT15-21 C57BL6 male mice subjected to similar handling procedures as cerebral ischemia mice. All values are mean ± SEM, n= 5 mice per group, comparisons via 2-tailed t test.

Supplementary Material

Refer to Web version on PubMed Central for supplementary material.

ACKNOWLEDGMENTS:

This study was supported in part by grants from the Rappaport Foundation (EHL), the Chinese Ministry of Education (XJ), and the National Research Foundation of Korea (JHP). The authors thank Jonathan Lipton, MingMing Ning and Wenjun Deng for helpful discussions, and Yihong Sun and all team members of the MGH 149-8 animal facility for help with light schedule switching.

Data availability.

The datasets generated during and/or analyzed during the current study are available from the corresponding author on reasonable request. Raw data associated with Figures and Extended Data are available via a source data file submitted with this manuscript.

REFERENCES:

1. Logan RW & McClung CA Rhythms of life: circadian disruption and brain disorders across the lifespan. Nat. Rev. Neurosci 20, 49–65 (2019). [PubMed: 30459365]
2. Cederroth CR et al. Medicine in the fourth dimension. Cell. Metab 30, 238–250 (2019). [PubMed: 31390550]
3. Ali M & Lees KR Personal communication, VISTA Database (2019).
4. Ding J et al. The effect of normobaric oxygen in patients with acute stroke: a systematic review and meta-analysis. Neurol. Res 40, 433–444 (2018). [PubMed: 29600891]
5. Green AR, Ashwood T, Odergren T & Jackson DM Nitrones as neuroprotective agents in cerebral ischemia, with particular reference to NXY-059. Pharmacol. Ther 100, 195–214 (2003). [PubMed: 14652110]
6. Schurr A Neuroprotection against ischemic/hypoxic brain damage: blockers of ionotropic glutamate receptor and voltage sensitive calcium channels. Curr. Drug Targets 5, 603–618 (2004). [PubMed: 15473250]
7. Neuhaus AA, Couch Y, Hadley G & Buchan AM Neuroprotection in stroke: the importance of collaboration and reproducibility. Brain 140, 2079–2092 (2017). [PubMed: 28641383]
8. Campbell BC, Meretoja A, Donnan GA & Davis SM Twenty-Year History of the Evolution of Stroke Thrombolysis With Intravenous Alteplase to Reduce Long-Term Disability. Stroke 46, 2341–2346 (2015). [PubMed: 26152294]
9. Campbell BCV et al. Endovascular stent thrombectomy: the new standard of care for large vessel ischaemic stroke. Lancet Neurol. 14, 846–854 (2015). [PubMed: 26119323]
10. Pritchett D & Reddy AB Circadian Clocks in the Hematologic System. J. Biol. Rhythms 30, 374–388 (2015). [PubMed: 26163380]
11. Schulz JB et al. Facilitation of postischemic reperfusion with alpha-PBN: assessment using NMR and Doppler flow techniques. Am. J. Physiol 272, H1986–1995 (1997). [PubMed: 9139987]
12. Buchan A & Pulsinelli WA Hypothermia but not the N-methyl-D-aspartate antagonist, MK-801, attenuates neuronal damage in gerbils subjected to transient global ischemia. J. Neurosci 10, 311–316 (1990). [PubMed: 2405111]
13. Lo EH A new penumbra: transitioning from injury into repair after stroke. Nat. Med 14, 497–500 (2008). [PubMed: 18463660]
14. Donnan GA, Baron JC, Ma H & Davis SM Penumbral selection of patients for trials of acute stroke therapy. Lancet Neurol. 8, 261–269 (2009). [PubMed: 19233036]
15. Heiss WD Experimental evidence of ischemic thresholds and functional recovery. Stroke 23, 1668–1672 (1992). [PubMed: 1440719]
16. Hossmann KA Viability thresholds and the penumbra of focal ischemia. Ann. Neurol 36, 557–565 (1994). [PubMed: 7944288]
17. Mure LS et al. Diurnal transcriptome atlas of a primate across major neural and peripheral tissues. Science 359 (2018).
18. Chen CY et al. Effects of aging on circadian patterns of gene expression in the human prefrontal cortex. Proc. Natl. Acad. Sci 113, 206–211 (2016). [PubMed: 26699485]
19. Balsalobre A et al. Resetting of circadian time in peripheral tissues by glucocorticoid signaling. Science 289, 2344–2347 (2000). [PubMed: 11009419]
20. Fan J, Dawson TM & Dawson VL Cell death mechanisms of neurodegeneration. Adv. Neurobiol 15, 403–425 (2017). [PubMed: 28674991]
21. Lipton P Ischemic cell death in brain neurons. Physiol. Rev 79, 1431–1568, (1999). [PubMed: 10508238]
22. Marshall JW, Duffin KJ, Green AR & Ridley RM NXY-059, a free radical--trapping agent, substantially lessens the functional disability resulting from cerebral ischemia in a primate species. Stroke 32, 190–198 (2001). [PubMed: 11136936]
23. Marshall JW, Cummings RM, Bowes LJ, Ridley RM & Green AR Functional and histological evidence for the protective effect of NXY-059 in a primate model of stroke when given 4 hours after occlusion. Stroke 34, 2228–2233 (2003). [PubMed: 12920263]

24. Paschos GK & FitzGerald GA Circadian clocks and vascular function. Circ. Res 106, 833–841 (2010). [PubMed: 20299673]

25. Durgan DJ, Crossland RF & Bryan RM Jr. The rat cerebral vasculature exhibits time-of-day-dependent oscillations in circadian clock genes and vascular function that are attenuated following obstructive sleep apnea. J Cereb Blood Flow Metab. 37, 2806–2819 (2017). [PubMed: 27798273]

26. Musiek ES et al. Circadian clock proteins regulate neuronal redox homeostasis and neurodegeneration. J. Clin. Invest 123, 5389–5400 (2013). [PubMed: 24270424]

27. Kobayashi Y, Ye Z & Hensch TK Clock genes control cortical critical period timing. Neuron 86, 264–275 (2015). [PubMed: 25801703]

28. Banks WA From blood-brain barrier to blood-brain interface: new opportunities for CNS drug delivery. Nat. Rev. Drug Discov 15, 275–292 (2016). [PubMed: 26794270]

29. Lo EH, Dalkara T & Moskowitz MA Mechanisms, challenges and opportunities in stroke. Nat. Rev. Neurosci 4, 399–415, doi:10.1038/nrn1106 (2003). [PubMed: 12728267]

30. Shi L et al. A new era for stroke therapy: Integrating neurovascular protection with optimal reperfusion. J. Cereb. Blood Flow Metab 38, 2073–2091 (2018). [PubMed: 30191760]

References for Methods:

31. Poli S & Veltkamp R Oxygen therapy in acute ischemic stroke - experimental efficacy and molecular mechanisms. Curr. Mol. Med 9, 227–241 (2009). [PubMed: 19275631]

32. Buchan AM, Slivka A & Xue D The effect of the NMDA receptor antagonist MK-801on cerebral blood flow and infarct volume in experimental focal stroke. Brain Res. 574, 171–177 (1992). [PubMed: 1386274]

33. Cao X & Phillis JW alpha-Phenyl-tert-butyl-nitrone reduces cortical infarct and edema in rats subjected to focal ischemia. Brain Res. 644, 267–272 (1994). [PubMed: 8050038]

34. Pschorn U & Carter AJ The influence of repeated doses, route and time of administration on the neuroprotective effects of BIII 277 CL in a rat model of focal cerebral ischemia. J. Stroke Cerebrovasc. Dis 6, 93–99 (1996). [PubMed: 17894976]

35. Folbergrova J, Zhao Q, Katsura K & Siesjo BK N-tert-butyl-alpha-phenylnitrone improves recovery of brain energy state in rats following transient focal ischemia. Proc. Natl. Acad. Sci 92, 5057–5061 (1995). [PubMed: 7761448]

36. Reimherr FW, Wood DR & Wender PH The use of MK-801, a novel sympathomimetic, in adults with attention deficit disorder, residual type. Psychopharmacol. Bull 22, 237–242 (1986). [PubMed: 3523579]

37. Shuaib A et al. NXY-059 for the treatment of acute ischemic stroke. N. Engl. J. Med 357, 562–571 (2007). [PubMed: 17687131]

38. Vinall PE, Kramer MS, Heinel LA, Rosenwasser RH Temporal changes in sensitivity of rats to cerebral ischemic insult. J. Neurosurg 93, 82–89 (2000).

39. Tischkau SA, Cohen JA, Stark JT, Gross DR, Bottum KM Time-of-day affects expression of hippocampal markers for ischemic damage induced by global ischemia. Exp. Neurol 208, 314–322 (2007). [PubMed: 17936274]

40. Becker MC et al. , Time-of-day dependent neuronal injury after ischemic stroke: implication of circadian clock transcriptional factor Bmal1 and survival kinase Akt. Mol. Neurobiol 55, 2565–2576 (2018). [PubMed: 28421530]

41. Ali K, Cheek E, Sills S, Crone P, Roffe C Day-night differences in oxygen saturation and the frequency of desaturations in the first 24 hours in patients with acute stroke. J. Stroke Cerebrovasc. Dis 16, 239–244 (2007). [PubMed: 18035240]

42. Kim BJ et al. Ischemic stroke during sleep – its association with worse early functional outcome. Stroke 42, 1901–1906 (2011). [PubMed: 21546480]

43. Karmarkar SW & Tischkau SA Influences of the circadian clock on neuronal susceptibility to excitotoxicity. Frontiers Physiol. 4, 313 (2013).

44. Ang TA et al. Circadian rhythm of redox state regulates excitability in suprachiasmatic nucleus neurons. Science 337, 839–842 (2012). [PubMed: 22859819]

45. Ghorbel MT, Coulson JM, Murphy D Crosstalk between hypoxic and circadian pathways – cooperative roles for HIF1-alpha and CLOCK in transcriptional activation of the vasopressin gene. Mol. Cell. Neurosci 22, 396–404 (2003). [PubMed: 12691740]

46. Lorenzano S et al. Early molecular oxidative stress biomarkers of ischemic penumbra in acute stroke. Neurology 93, 1288–1298 (2019).

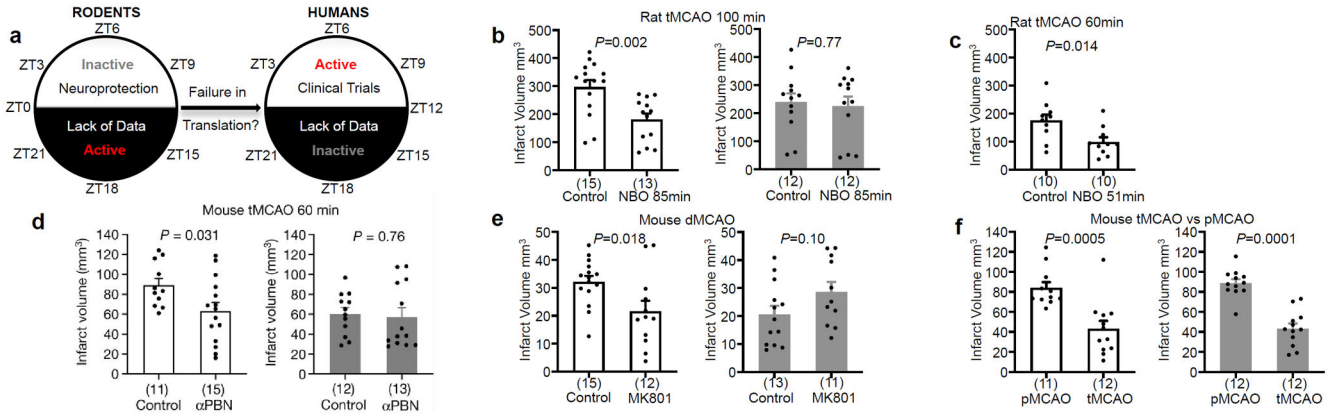

Figure 1. Neuroprotection in rodent models of stroke.

a. Opposite circadian cycles in nocturnal rodents versus diurnal humans. **b.** 100 min middle cerebral artery occlusion (MCAO) in male Sprague-Dawley rats. Controls received 30% O_2. NBO group received 100% O_2 (for 85% of ischemic period). NBO reduced infarction at ZT3-9 but not ZT15-21. **c.** NBO (for 85% of ischemic period) reduced infarction after 60 min MCAO in Sprague-Dawley rats during ZT3-9. **d.** αPBN (100 mg/kg IP immediately and 2 hrs post-reperfusion) reduced infarction after 60 min MCAO in ZT3-9 but not ZT15-21 mice. **e.** MK801 (2.5 mg/kg IP, 1 hr pre-occlusion) reduced infarction after permanent MCAO in ZT3-9 but not ZT15-21 mice. **f.** Infarct volumes were smaller in 60 min transient versus permanent MCAO in both ZT3-9 and ZT15-21 mice. All values in Figure 1 are mean ± SEM; comparisons via 2-tailed t-test. Physiologic parameters, laser-doppler flow, inclusion/exclusion/mortality in Extended Data 1. White bars: ZT3-9; gray bars: ZT15-21. Infarct volumes quantified with triphenyltetrazolium (TTC) staining. (n) indicate animals per group. tMCAO: transient MCAO; pMCAO: permanent MCAO; dMCAO permanent distal MCAO.

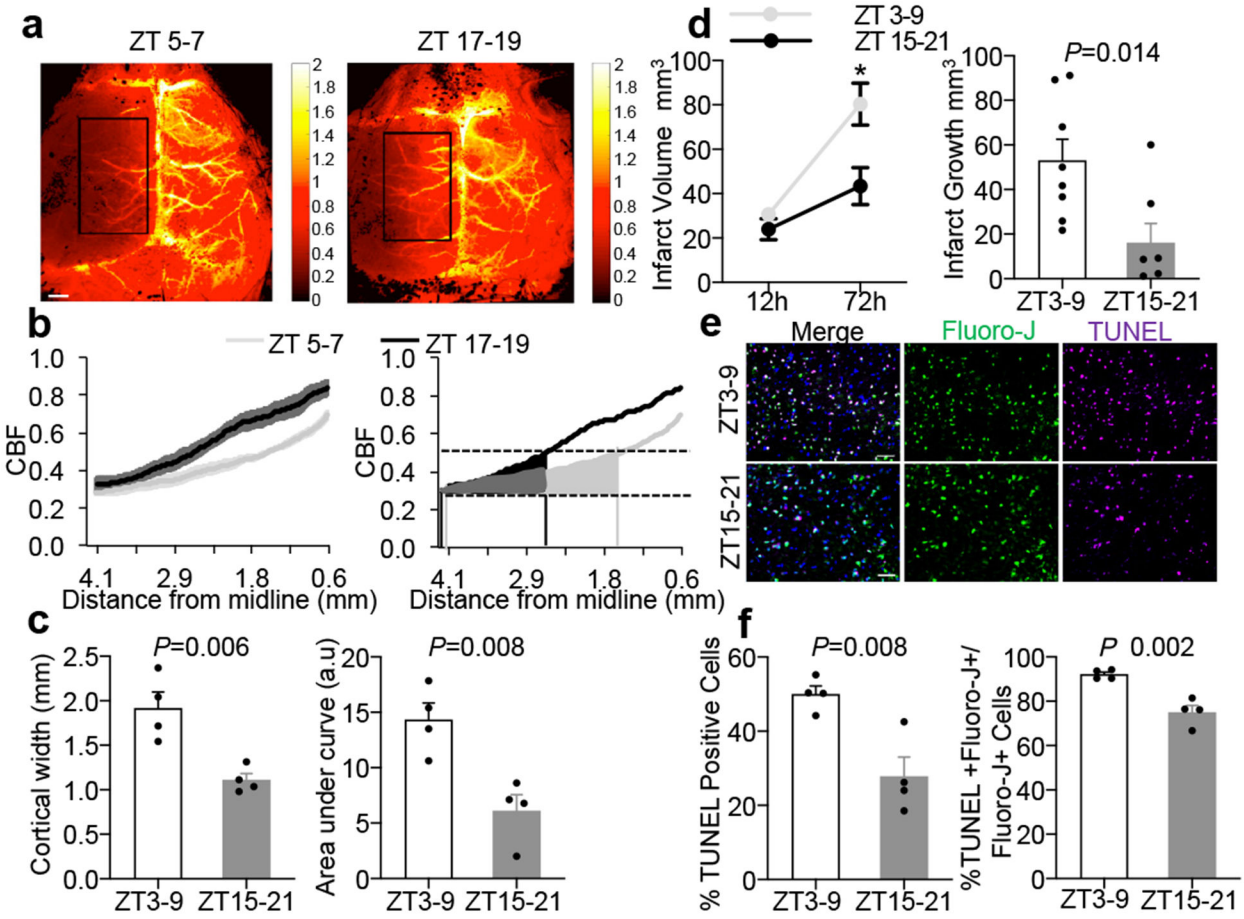

Figure 2. Comparisons of penumbra after focal cerebral ischemia.

a. Laser speckle imaging at 25 mins post-MCAO in ZT5-7 versus ZT17-19 C57BL6 mice. Rectangular area for quantifying data from 4 independent experiments/mice per group in (b) and (c). Scale: 1 mm. **b.** Ipsilateral blood flow gradients were steeper in ZT17-19 versus ZT5-7 images (line is mean, shaded areas are SEM, left panel; area-under-curve, right panel). **c.** The blood flow penumbra was operationally defined as average cortical width or area-under-curve between 30-50% of normal levels, based on a lower threshold of infarction and an upper threshold of gene expression and protein synthesis inhibition (25-55 mL/100g/min, see Methods and References[15,16]). The penumbra was narrower in ZT17-19 versus ZT5-7 mice. Physiologic parameters were similar across all animals (Extended Data 5). Penumbral perfusion was not correlated with blood pressure or pCO_2 (r^2 = 0.006 and 0.171 respectively). **d.** Infarct growth (12 to 72 hrs) after 60 min MCAO was smaller in ZT15-21 (n=8) versus ZT3-9 (n=9) mice. **e.** Representative TUNEL, fluoro-jade and DAPI immunostaining in penumbral cortex at 24 hrs after 60 min MCAO in mice. Scale: 50 μm. **f.** Percentages of TUNEL/DAPI and TUNEL plus fluoro-jade/fluoro-jade were lower in ZT15-21 versus ZT3-9 penumbra (n=4 mice per group). All values in Figure 2 are mean ± SEM; comparisons via 2-tailed t-test.

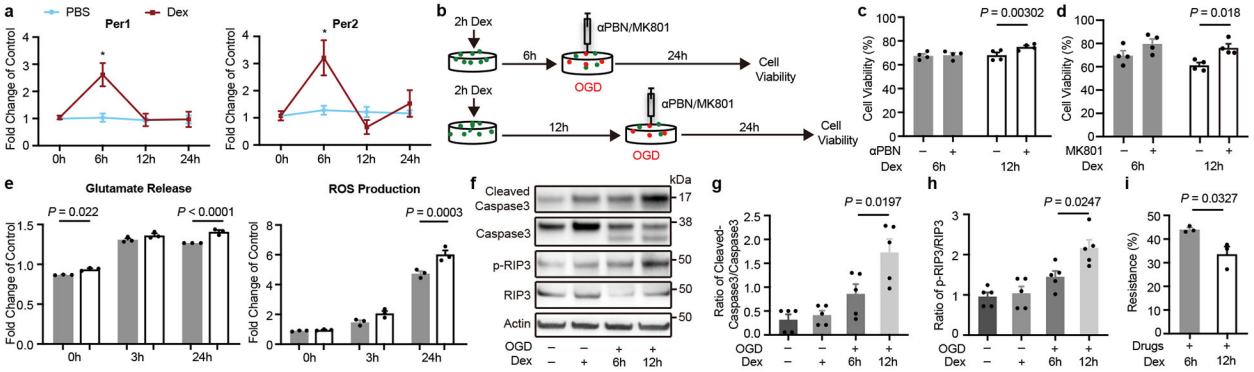

Figure 3. Effects of circadian cycles on response to oxygen-glucose deprivation and neuroprotection.

a. Primary mouse cortical neurons were treated for 2 hrs with dexamethasone (Dex). Per1/2 levels at 6 and 12 hrs matched in vivo circadian cycles for rats and mice at ZT15-21 (upregulated Per1/2) and ZT3-9 (downregulated Per1/2). *P=0.0003 (Per1), *P=0.0026 (Per2), n=3 independent experiments in triplicate. **b.** Oxygen-glucose deprivation (OGD) with αPBN or MK801 in neurons after induction of circadian-like cycles in vitro. **c.** αPBN was neuroprotective when Per1/2 were downregulated (n=4 independent experiments in triplicate). **d.** MK801 was neuroprotective when Per1/2 were downregulated (n=4 independent experiments in triplicate). **e.** After 3 hrs OGD, glutamate release and ROS production were lower during times with upregulated Per1/2 (n=3 independent experiments in triplicate). **f.** Representative western blots of cleaved caspase-3, caspase-3, phosphorylated RIP3 kinase and RIP3 kinase at 24 hrs after OGD (gel source data in Supplementary Information; n=5 independent experiments for densitometry). **g.** Quantitation of cleaved caspase-3/caspase-3. **h.** Quantitation of phosphorylated RIP3 kinase/RIP3 kinase. **i.** “Resistance to neuroprotection” after combination treatment with MK801 (10 μM), NBQX (50 μM), αPBN (1μM), zVAD-fmk (50 μM) and Necrostatin-1 (100 μM) (n=3 independent experiments in triplicate). All data in Figure 3 are mean ± SEM; two-way ANOVA with Bonferroni adjustment (**a, c, d, e)** or one-way ANOVA with post-hoc Tukey adjustment (**g, h**) or unpaired 2-tailed t-test (**i**).